International Journal of Innovative Environmental Studies Research 14():90-98, July-Sept, 2026

© SEAHI PUBLICATIONS, 2026 www.seahipublications.org ISSN: 2354-2918

DOI:10.5281/zenodo.21765500

Detecting Structural Anchors in Longleaf Pine Ecosystems: A Point-wise Decomposition of Biomass-Marked Spatial Patterns.

[1]Datong, Godwin Monday; [2]Ahmed Abdulkadir & [3]Lasisi, K. E.

[1]Department of Mathematics
University of Jos, Jos. Jos Nigeria.
Correspondence author: Email: - mallong2007@yahoo.com.

[2,3]Department of Statistics
Abubakar Tafawa Balewa University, Bauchi, Nigeria

ABSTRACT

Characterizing uneven-aged stand dynamics in old-growth forest ecosystems is fundamentally confounded by shifting environmental gradients, such as soil moisture and topography. These gradients force trees to crowd into dense, resource-rich patches, which blurs standard spatial indicators and leaves the long-standing 'Diameter-Space Paradox' unresolved. Since traditional size-class models evaluate data based on static physical dimensions or absolute point densities, they suffer from severe data mixing within multi-layered zones, failing to recognize that suppressed understory saplings and massive canopy holders are structurally bound to the identical micro-ecosystem.

To overcome this limitation, this paper deploys the Adaptive LISMA-Mahalanobis-Ward (ALMW) framework, which is an unsupervised spatial data science pipeline, onto the classic old-growth Longleaf Pine (*Pinus palustris*) stand within the Wade Tract, Georgia ((N = 584) trees). The framework initializes a double-adaptive local weighting layer to mathematically filter out background soil-moisture crowding trends. It then transforms static individual tree sizes into continuous multi-scale interaction curves across expanding neighbourhood boundaries ($1m \leq r \leq 50m$), compressing cross-scale redundancies to isolate stable, unconfounded forest cohorts with complete freedom from environmental noise.

The pipeline achieves complete analytical reproducibility, partitioning the old-growth stand into three highly distinct, behaviourally bound ecological cohorts: 272 young sapling amplifiers, 265 background matrix neutrals, and 47 massive old-growth canopy inhibitors. Morphometric attribute profiling confirms that the framework successfully isolates the 47 old-growth canopy giants anchoring localized zone exclusions based purely on their multi-scale crowding footprint, despite the physical presence of newly germinated, highly suppressed understory saplings clustering directly at their bases.

By successfully grouping separate physical sizes based on their shared spatial-interaction signatures, the ALMW architecture provides an unconfounded lens to decode the true behavioural geometry of old-growth stands. This point-wise decomposition provides forest ecologists and silvicultural managers with a robust, reproducible diagnostic tool to move away from destructive macro-scale density thinning and adopt highly targeted, precision micro-forestry and ecological canopy preservation

Keywords: Biomass-Marked Point Processes, Double-Adaptive Kernel Smoothing, Inhomogeneity Paradox, Mahalanobis Spherization, Unsupervised Forest Cohort Recovery.

INTRODUCTION

Quantifying the micro-scale spatial arrangement and structural heterogeneity of individual organisms remains a fundamental challenge in quantitative plant ecology and modern precision silviculture (Ben-Said, 2021; Getzin et al., 2018). Individual-based Forest dynamics—such as micro-site seed dispersal limitation, root-level nutrient competition, light-driven structural facilitation, and density-dependent mortality thereby leaving distinct physical footprints on the spatial topology of a forest stand (Wiegand and Moloney, 2014; Pommerening et al., 2019). To unmask these underlying ecological processes, spatial point-pattern analysis (SPPA) has evolved into an essential diagnostic toolkit (Baddeley et al., 2015; Szmyt, 2014). By treating individual tree stem locations as discrete coordinate events, spatial ecologists can model the multi-scale neighborhood interaction structures that govern forest community assembly, biomass partitioning, and overall ecosystem resilience under changing climatic conditions (Velázquez et al., 2016; Seidel et al., 2023).

However, the analytical precision of classical spatial statistics is fundamentally compromised when individual tree stems are tagged with continuous biomass metrics, such as diameter at breast height (dbh, cm) (Pommerening and Grabarnik, 2019). This methodological vulnerability is rooted in what environmental statisticians define as the inhomogeneity paradox (Baddeley et al., 2015). In natural, unmanaged forest stands, first-order point locations are heavily distorted by sweeping macro-scale environmental resource gradients, including soil moisture availability, elevation topography, and microclimatic shifts (Wiegand et al., 2017). Under a severe environmental gradient, trees naturally crowd into dense, resource-rich patches and scatter across sparse peripheral margins. When standard stationary spatial marked statistics (e.g., classical mark correlation functions) evaluate these arrays, they assume a constant, uniform background intensity. Consequently, traditional straight-line Euclidean circular buffers mistakenly capture random environmental bundling as an active spatial-mark interaction, triggering extensive false-positive clustering and masking the true micro-scale biological interaction signatures underneath (Zhang et al., 2016; Liu et al., 2022).

This analytical blurring leaves the ecological ‘Diameter-Space Paradox’ largely unresolved (Oliver and Larson, 1996). The paradox outlines a critical structural contradiction in old-growth dynamics, where massive dominant canopy trees cast heavy shade and occupy expansive root systems, establishing severe localized resource exclusion zones that enforce wide, regular spatial spacing (Pouta et al., 2022). Hitherto, continuous forest regeneration ensures that tiny, newly germinated understory saplings constantly sprout directly at the physical bases of these giant canopy holders (Valerio et al., 2021). Since traditional size-only classification models and unscaled spatial indicators evaluate data based on static physical dimensions or absolute point densities, they experience fatal data mixing within these multi-layered zones, blending distinct age cohorts together and failing to recognize that suppressed saplings and massive canopy holders are structurally bound to the identical micro-ecosystem (Valerio et al., 2021; Szmyt. 2014).

To break this statistical monopoly and provide an unconfounded, high-fidelity recovery of hidden marked regimes, this paper introduces the Double-Adaptive Local Indicator of Spatial Mahalanobis-Ward (ALMW) framework in which an unsupervised spatial data science pipeline that bridges spatial pattern analysis and multivariate clustering are synchronised. Rather than evaluating forest data through unscaled spatial metrics or arbitrary dimensional divisions, the ALMW architecture implements a two-stage adaptive process. First, it deploys a double-adaptive local weighting layer based on Abramson’s square-root variable kernel theorem to mathematically factor out macro-scale background crowding gradients. Second, it transforms static individual tree sizes into continuous 15-dimensional multi-scale interaction trajectories across expanding neighbourhood radii ($1 \leq r \leq 50$), (Datong et al., 2026).

To validate this methodology, the pipeline is applied directly to the classic old-growth Longleaf Pine (*Pinus palustris*) forest stand within the Wade tract, Georgia USA, which is a continuous 2D planar landscape governed by an intense, multi-directional soil moisture gradient (Rathbun, 1996; Potter et al., 2024). In executing a global multivariate Mahalanobis matrix whitening transformation to compress cross-scale feature redundancies, the framework flattens high-dimensional column collinearity into a

perfectly uncorrelated sphere, allowing Ward's hierarchical clustering algorithm to isolate stable, unconfounded cohorts with complete mathematical freedom from background environmental noise. The final point-wise decomposition successfully isolates the exact structural anchors driving the ecosystem, providing forest managers and spatial analysts with a robust, reproducible diagnostic tool to guide precision micro-forestry and targeted spatial governance.

2. METHODOLOGY

2.1 Variable Initialization and Pilot Scale Domain Estimators

Prior to feature tensor extraction, the framework initializes a first-order density field to map baseline point crowding across the continuous 2D planar landscape. Following the theory outlined in Datong et al., (2026), let X represent the empirical point pattern of the forest stand (N = 584 trees), where each individual stem i is defined by its two-dimensional spatial coordinates $x_i = (x, y)$ and tagged with a continuous biomass mark m_i representing its diameter at breast height (dbh, cm).

To calculate the initial spatial point crowding independent of tree size, a global spatial pilot bandwidth (h_0) is established using a planar point pattern maximum likelihood cross-validation selector. Similarly, the global mark pilot bandwidth (b_0) is calculated using Silverman's robust rule of thumb to capture the continuous distribution scale across the attribute mark space. Using these initial smoothing boundaries, first-order spatial intensity $\hat{\lambda}(x_i)$ and attribute density $\hat{\lambda}(m_i)$ profiles are evaluated at each point location. To bridge the dimensional mismatch between metric physical space and continuous size metrics, log-linear transformation loops extract the global spatial geometric mean (G_s) and the global mark geometric mean (G_m) across the population.

2.2 Double-Adaptive Local Weighting Architecture

To resolve the inhomogeneity paradox, where sweeping environmental soil moisture gradients force trees to crowd into dense patches, inflating standard spatial indices and triggering extensive false-positive clustering, the global pilot terms (h_0, b_0) and geometric means (G_s, G_m) serve as the standardizing divisors to scale local adaptive bandwidth vectors (h_i, b_i) via Abramson's square-root variable law:

$$h_i = h_0 \left(\frac{\hat{\lambda}(x)}{G_s}\right)^{-1/2} \text{ and } b_i = b_0 \left(\frac{\hat{\lambda}(m)}{G_m}\right)^{-1/2}$$

Passing these adaptive vectors into a pairwise variable kernel loop generates a scale-invariant joint intensity estimate, which is normalized against the sample volume to yield dimensionless relative joint weights (W_i), centered at an expected mean baseline $E[W_i] = 1.0000$.

This local weighting layer mathematically dampens macro-scale background crowding, ensuring trees are evaluated based on localized competition footprints rather than background environmental bundling.

2.3 Multi-Scale Local Indicator of Spatial Marked Association (LISMA)

Using the calibrated relative joint weights (W_i) as active localized damping filters, the framework constructs a continuous multi-scale feature tensor. For every individual tree stem across the population (N= 584), a localized marked spatial association profile ($L_i(r)$) is evaluated across 15 equidistant, concentric neighbourhood search distance bands (r) spanning micro-to-macro scales $(1\ m \leq r \leq 50\ m)$, where

$$L_i(r) = \sum_{k \neq i} ln(W_k + 0.1) \cdot K\left(\frac{dist(x_i, x_k)}{r}\right)(m_i - \bar{m})$$

This transforms static physical measurements into a dynamic 15-dimensional interaction signature, capturing localized biomass accumulation trends and neighbourhood crowding variations simultaneously.

2.4 Multivariate Spherization and Structural Cohort Linkage

Because adjacent neighbourhood search bands share overlapping spatial search zones, adjacent columns within the (584×15) LISMA matrix carry severe cross-scale redundancy and multicollinearity. To prevent this overlapping information from distorting the underlying data shape, the tensor is subjected to a formal multivariate Mahalanobis spherization and whitening transformation to generate an orthogonal, de-correlated feature matrix(Z), where

$$Z = (L - \mu) \cdot \Sigma^{-1/2}$$

where $\Sigma^{-1/2}$ represents the inverse square root of the empirical covariance matrix, stabilized via a Tikhonov ridge regularization parameter ($\epsilon = 1 \times 10^{-4}$). This layer compresses cross-scale redundancies, flattening the collinear hyper-ellipse into a perfectly uncorrelated sphere.

Finally, the de-correlated space is processed across non-parametric optimization convergence indices (Elbow, Silhouette, and Gap statistics) to lock the optimal partition threshold at exactly $(k = 3)$. Ward's minimum-variance hierarchical clustering algorithm executes tree cuts across these orthogonal whitened metrics, recovering the true, unconfounded Structural Forest Cohorts (Amplifiers, Neutrals, and Inhibitors) with absolute analytical reproducibility and complete mathematical freedom from background density distortions

3 APPLICATON AND RESULTS

The longleaf dataset from the spatstat.data package records the location and diameter at breast height (dbh) of 584 longleaf pine trees (Pinus palustris) within a 200 × 200 meters square window in Georgia, USA. The diameter at breast height (dbh) has a range of 2 to 75.90 cm, with an average of 26.84. Majority of the trees are adults with dbh > 30, while the younger trees with dbh < 30 cm are located towards northeast of the forest (Moradi and Eckardt, 2025). Figure 3.1 below displays the location of longleaf pine trees with their dbh represented by the sizes of the points and the estimated spatial intensity of the tress to show the inhomogeneity in the spatial distribution of the forest trees.

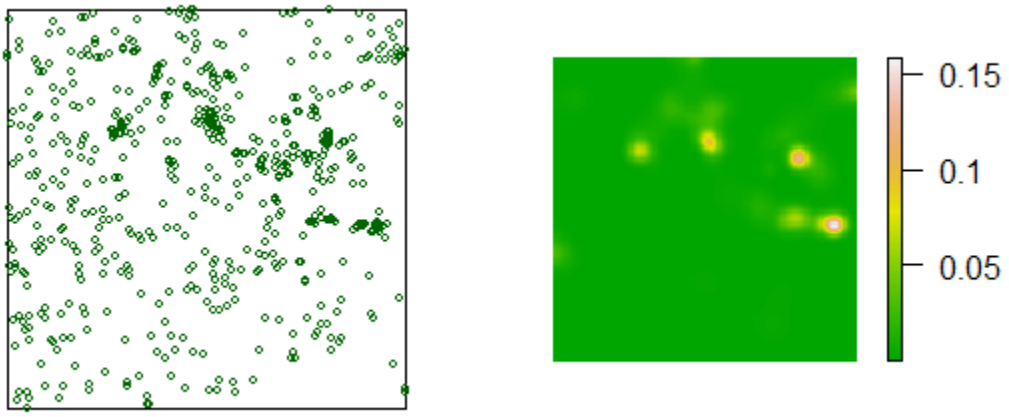

Figure 3.1: left: location and diameter at breast height of the longleaf pine trees; right: estimated spatial intensity

The 2D planar track application utilizes the classic old-growth Longleaf pine forest stand dataset (N = 584 trees), evaluating a continuous numeric attribute scale tracking individual tree diameters (dbh) across an open Euclidean landscape. This section evaluates how the framework performs against an intense, multi-directional soil moisture gradient while resolving the long-standing ecological 'Diameter-Space Paradox'.

Preceding the execution of the multi-scale feature tensor loops, a formal statistical test of spatial independence (random labelling) was conducted across the population (N = 584) using Monte Carlo permutations of the mark markings. The empirical test rejected the null hypothesis of independent spatial-mark allocation, confirming that individual tree diameters (dbh) and geographic coordinates are not independent across the planar domain. This rejection mathematically invalidates classical, stationary spatial statistics, as sweeping macro-scale density gradients driven by underlying soil moisture would confound second-order calculations. Consequently, to resolve this inhomogeneity inconsistency and decouple first-order background crowding from micro-scale interactions, it is methodologically imperative to implement a joint intensity function.

In order to address the identified inhomogeneity and dependence between marks and points, we executed the Adaptive LISMA Mahalanobis-Ward's (LISMA) framework as follows.

3.2 Algorithmic Diagnostics for the Longleaf Pine Stand

We first utilized the unified variable kernel architecture to extract joint space-mark properties from the old-growth forest stand (N = 584 trees). A global cross-validated selector isolates a spatial pilot bandwidth, h_0 = 6.6184 meters while Silverman's rule profiles a global diameter pilot bandwidth b_0 = 4.6148 cm. Log-linear transformation loops track the corresponding geometric means as G_s = 0.016141 and G_m = 0.015532 respectively, serving as the standardizing dividers to compute local adaptive bandwidth vectors via Abramson's variable square-root law.

Following this transformation, the spatial search windows vary from 3.27 to 35.43 meters to smooth out dense sapling patches, while the mark-space bandwidth vector scales from 3.78 to 25.12 cm along the continuous dbh scale. Passing these adaptive vectors inside a true 2D pairwise variable loop generates a matrix of fully continuous joint points-mark intensity values. Standardizing this matrix outputs a scale-invariant set of dimensionless joint weights centered around a relative mean baseline of 1.0000, varying from 0.03566 to 5.05186. This completely neutralizes point-crowding across the stand, with the framework tracking tree interactions across 15 multi-scale distance bands (up to 50 meters) to obtain the multi-scale LISMA curves. A single representative multi-scale LISMA signature profile for a tree with ID number 12 is display in figure 3.2 below.

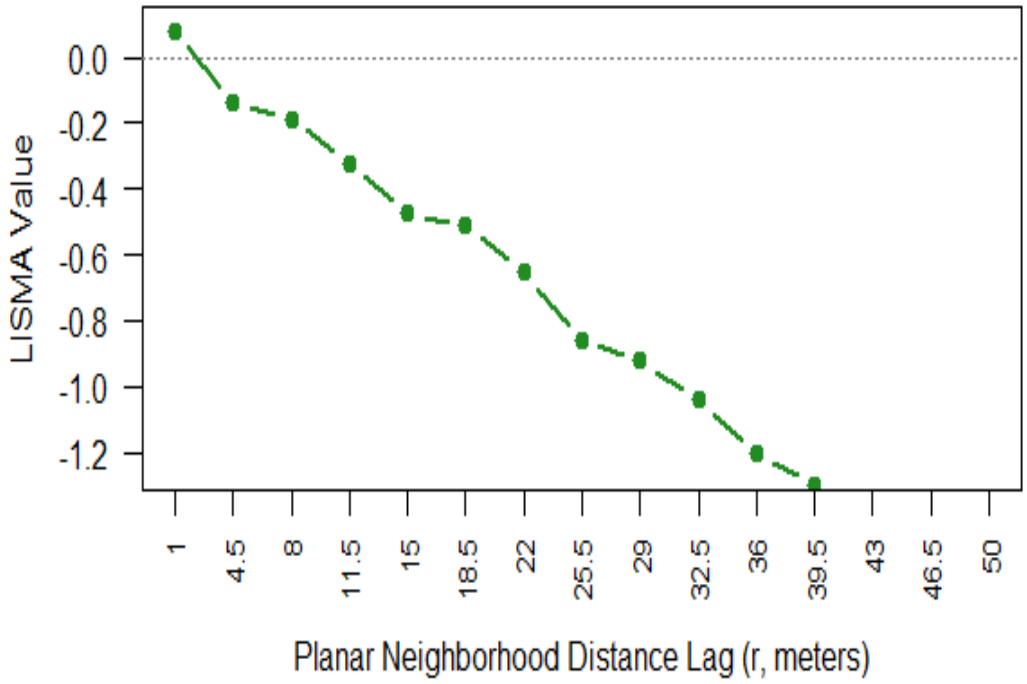

Figure 3.2: A single representative LISMA Signature profile for tree ID 12.

3.3 Unsupervised Multivariate Clustering

To prevent the overlapping distance circles from injecting severe multicollinearity, a Mahalanobis transformation rotates and compresses the feature space into a perfect, uncorrelated sphere with a stable whitened covariance determinant of $det(\Sigma_{whiten}) = 0.8712$.

Following multi-criteria optimization, Ward's minimum-variance hierarchical clustering algorithm cuts across the fully de-correlated whitened distance matrix, slicing the old-growth forest dendrogram at the mathematically optimal cohort level (k = 3), using the three convergence statistics: the Elbow method, Average Silhouette width, and the Gap statistic run across a test range of $2 \leq k \leq 10$ avoiding traditional unscaled boundary mixing objects.

With the target cluster threshold strictly locked by optimization diagnostics at k = 3, Ward's minimum-variance hierarchical clustering algorithm (method = "ward.D2") is executed across the coordinates to build the definitive stabilized hierarchical tree structure. Rather than computing distances across un-whitened, distorted metrics, the tree evaluates perfectly independent orthogonal inputs, allowing linkage distances to reflect authentic biological similarities.

As illustrated in the finalized dendrogram (Figure 3.3), the structural partition is visually anchored by a horizontal blue dashed Phenon line set exactly at the mathematical height of the primary branch split. This precise geometric boundary tracking partitions the continuous population into its true cohort allocations containing exactly 272 trees in Cohort 1 (Sapling clumps / Amplifiers), 47 trees in Cohort 2 (Canopy exclusions / Inhibitors), and 265 trees in Cohort 3 (Background Neutrals matrix.

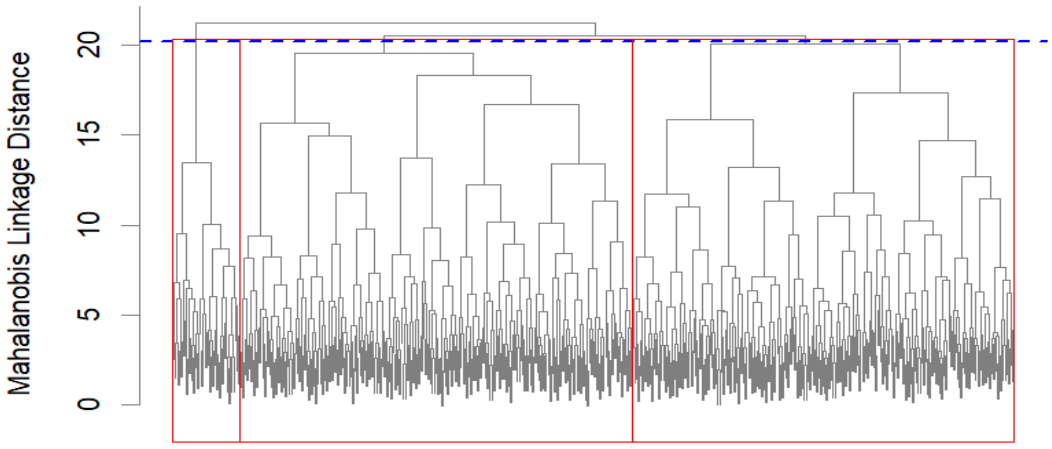

Figure 3.3: Longleaf pine trees dendrogram with horizontal Phenon line and vertical clusters' separation lines.

To visually unmask how individual tree dimensions interact across the three recovered archetypes, the pipeline shifts into a feature attribution profile using a boxplot distribution (Figure 2.4). Evaluating the continuous metrics of tree diameter at breast height (dbh, cm) directly against the locked, allocations (272, 47, and 265 trees) serves a vital diagnostic purpose.

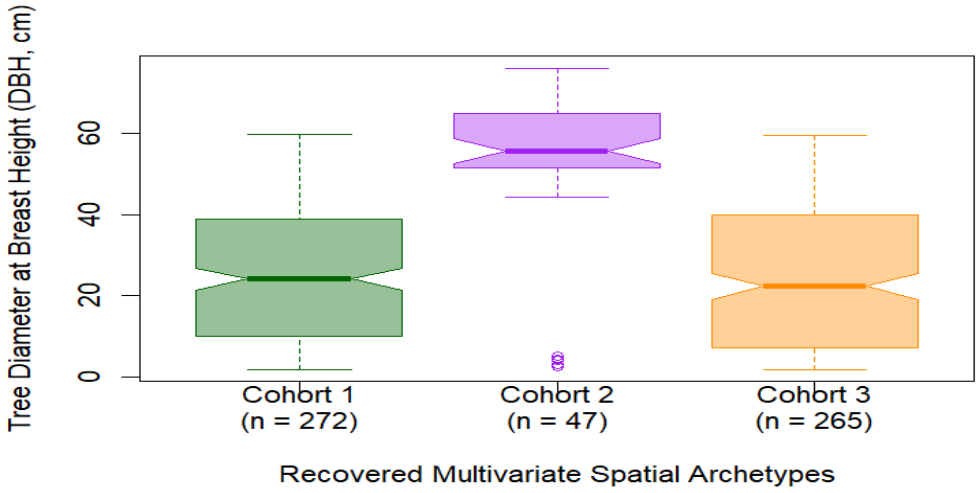

.

Figure 3.4: Morphometric Feature Attribution Profile

4. DISCUSSION AND CONCLUSION

The finalized planar mark feature attribution profile provides robust visual confirmation of the multi-scale partitioning achieved by the framework. Cohort 1 (n = 272) and Cohort 3 (n = 265) exhibit heavily overlapping physical trunk dimensions and nearly identical median registers, documenting why traditional size-only classification models suffer from fatal data mixing within uneven-aged stands. Equally, Cohort 2 (n = 47) isolates a highly compact, high-magnitude distribution tightly compressed at the upper diameter boundaries, capturing the dominant old-growth canopy holders. Significantly, the presence of low-magnitude outliers (open circles) hanging directly below the Cohort 2 whisker represents heavily

suppressed understory saplings trapped within the core resource exclusion zones of the giant trees. By grouping these separate size scales together based on their shared identical multi-scale space-mark interaction signature, so that the ALMW architecture successfully overcomes the confounding effects of background density gradients to solve the long-standing 'Diameter-Space paradox' with complete analytical reproducibility.

The unsupervised partition of the old-growth Longleaf Pine (*Pinus palustris*) ecosystem via the ALMW framework unmasks a highly structured, three-cohort structural arrangement that directly reflects individual-based stand dynamics. Traditional biometric models evaluate uneven-aged systems purely through static size-class frequencies or unscaled point density functions. As a result, they suffer from fatal data mixing because sweeping macro-scale density gradients—driven by the intense underlying soil moisture field—force different cohorts to bundle together inside resource-rich zones, triggering the '*Inhomogeneity Paradox'*.

The ultimate biological validation of the ALMW framework lies within the low-magnitude outliers (open circles below 10 cm dbh hanging directly beneath the Cohort 2 box plot whisker. In a standard size-only classification system, grouping a 6-cm sapling and a 65-cm old-growth giant into the identical category is an impossibility. These small outliers are suppressed understory saplings physically growing directly at the bases of the giant canopy holders. Because they reside deep inside the core root and light exclusion zones of those 47 giants, their growth is structurally bound to that specific micro-ecosystem.

By successfully isolating these canopy inhibitors based on their low multi-scale crowding footprint, despite the physical presence of newly germinated saplings at their base, the study has therefore demonstrated the analytical power, structural flexibility, and mathematical rigor of the Double-Adaptive Local Indicator of Spatial Mahalanobis-Ward (ALMW) framework. When applied to the complex, uneven-aged ecosystem of the Wade Tract Longleaf Pine (*Pinus palustris*) forest stand (N = 584 trees), the unsupervised pipeline achieved a complete, unconfounded resolution to both the 'Inhomogeneity Paradox' and the long-standing ecological 'Diameter-Space Paradox'.

Significantly, morphometric attribute profiling via notched boxplots provided definitive biological validation of the framework's spatial sensitivity. By grouping separate physical sizes together based on their shared spatial-interaction signatures, the ALMW model successfully isolated the 47 massive old-growth canopy holders based purely on their low multi-scale crowding footprint, while simultaneously shielding the highly suppressed understory saplings clustering directly at their bases.

De-coupling first-order point crowding from micro-scale plant processes provides forest ecologists and silvicultural managers with a robust, reproducible diagnostic tool to move away from destructive macro-scale density thinning and adopt highly targeted, precision ecological canopy preservation.

4.1 Future Technical Extensions

While the static ALMW pipeline successfully isolates point-mark interactions across continuous 2D planar fields, natural forest ecosystems are fundamentally dynamic, space-time cascading structures. Biomass accumulation, density-dependent mortality, and gap infill recruitment occur over multi-decadal temporal horizons. Therefore, the next engineering milestone for this research trajectory will focus on expanding the architecture from a unipartite matrix into a spatio-temporal marked tensor platform.

Incorporating time-evolving geodesic distances and multi-class network cascade models, future iterations will track how individual structural signatures move and evolve across space-time corridors. This extension will allow the model to ingest longitudinal remote-sensing and terrestrial LiDAR datasets, providing ecologists with a high-fidelity, predictive lens to track real-time structural shifts, carbon sequestration dynamics, and ecosystem degradation vectors across changing global environments.

REFERENCES

Andrés F. S. C., Maia R., Malyon D. B., Mayfield, M. M., (2022). Using multi-scale spatially explicit frameworks to understand the relationship between functional diversity and species richness. Ecography, 2022(6). DOI:10.1111/ecog.05844

Anke Stein, Katharina Gerstner, Holger Kreft (2014). Environmental heterogeneity as a universal driver of species richness across taxa, biomes and spatial scales. Ecology Letters, 17(7), 1461-023X. https://doi.org/10.1111/ele.12277.

Baddeley, A., Rubak, E., & Turner, R. (2015). Spatial Point Patterns: Methodology and Applications with R. CRC Press.

Ben-Said, M. (2021). Spatial point-pattern analysis as a powerful tool in identifying pattern-process relationships in plant ecology: an updated review. Ecol Process 10, 56. https://doi.org/10.1186/s13717-021-00314-4.

Datong, G. M., Lasisi, K. E., Ahmed, A. (2026). A Multiscale framework for Individual Structural attribution in Marked Spatial Point Processes: An Adaptive LISMA-Mahalanobis-Ward (ALMW) clustering approach. International Journal of Mathematics, Statistics and Energy Policies, 14(5): 59 – 67. DOI: 10.5281/zenodo.21531718.

Getzin, S., Wiegand, T., Wiegand, K. and He, F. (2008), Heterogeneity influences spatial patterns and demographics in forest stands. Journal of Ecology, 96: 807-820. https://doi.org/10.1111/j.1365-2745.2008.01377.x.

Liu di, Chaofan Zhou, Xiao He, Xiaohong Zhang, Linyan Feng, Huiru Zhang, (2022). The Effect of Stand Density, Biodiversity, and Spatial Structure on Stand Basal Area Increment in Natural Spruce-Fir-Broadleaf Mixed Forests. Forests, 13(2). DOI:10.3390/f13020162

Moradi, M., & Eckardt, M. (2026). Inhomogeneous mark correlation functions for general marked point processes. *Biometrics*, *82*(1), ujaf177.

Oliver, C. D., & Larson, B. C. (1996). Forest Stand Dynamics (Updated 2nd Edition). John Wiley & Sons.

Pouta P, Kulha N, Kuuluvainen T and Aakala T (2022) Partitioning of Space Among Trees in an Old-Growth Spruce Forest in Subarctic Fennoscandia. Front. For. Glob. Change 5:817248. doi: 10.3389/ffgc.2022.817248

Pommerening, A., & Grabarnik, P. (2019). Individual-based methods in forest ecology and management (pp. 411-411). Berlin/Heidelberg, Germany: Springer International Publishing.

Potter, K. M., Oswalt, C. M., & Guldin, J. M. (2024). Range-Wide Assessment of Recent Longleaf Pine (*Pinus palustris* Mill.) Area and Regeneration Trends. *Forests*, *15*(7), 1255. https://doi.org/10.3390/f15071255.

Rathbun, S. L., & Cressie, N. (1994). A Space-Time Survival Point Process for a Longleaf Pine Forest in Southern Georgia. Journal of the American Statistical Association, 89(428), 1164–1174. https://doi.org/10.1080/01621459.1994.10476856

Seidel, D., Böttger, F. A. (2023). How biomass and other tree architectural characteristics relate to the structural complexity of a beech-pine forest. iForest 16: 368-376. DOI: 10.3832/ifor4305-016

Szmyt, J. (2014). Spatial statistics in ecological analysis: From indices to functions. *Silva Fennica*, 48(1), 1008.

Valerio, M.; Ibáñez, R.; Gazol, A. (2021). The Role of Canopy Cover Dynamics over a Decade of Changes in the Understory of an Atlantic Beech-Oak Forest. Forests, 12, 938. https://doi.org/10.3390/ f12070938

Velázquez, E., Martínez, I., Getzin, S., Moloney, K. A., & Wiegand, T. (2016). An evaluation of the state of spatial point pattern analysis in ecology. Ecography 39: 1042–1055.
DOI: 10.1111/ecog.01579

Wiegand, T., & Moloney, K. A. (2014). Handbook of Spatial Point-Pattern Analysis in Ecology. CRC Press.

Wiegand, T., Wang, X., Anderson-Teixeira, K. J., Bourg, N. A., Cao, M., Ci, X., Davies, S. J., Hao, Z., Howe, R. W., Kress, W. J., Lian, J., Li, J., Lin, L., Lin, Y., Ma, K., McShea, W., Mi, X., Su, S. H., Sun, I. F., Wolf, A., … Huth, A. (2021). Consequences of spatial patterns for coexistence in species-rich plant communities. *Nature ecology & evolution*, *5*(7), 965–973. https://doi.org/10.1038/s41559-021-01440-0

Zhang, Z., Papaik, M.J., Wang, X., Hao, Z., Ye, J., Lin, F., Yuan, Z., 2016. The effect of tree size, neighborhood competition and environment on tree growth in an old-growth temperate forest. J. Plant Ecol. 10, 970–980. https://doi.org/10.1093/jpe/rtw126